Published in final edited form as:
J Immunol. 2008 June 15; 180(12): 7907–7918.

Central memory CD8+ T cells have a shorter lifespan and reduced abundance as a function of HIV disease progression[1]

Kristin Ladell[*,†], **Marc K. Hellerstein**[‡], **Denise Cesar**[‡], **Robert Busch**[§,¶], **Drina Boban**[‖], and **Joseph M. McCune**[2,*]

* *Division of Experimental Medicine, University of California at San Francisco, CA, USA*

‡ *Department of Nutritional Sciences, University of California at Berkeley, CA, USA*

§ *KineMed, Inc., Emeryville, CA, USA*

‖ *Department of Medicine, University of California at San Francisco, CA USA*

Abstract

Progressive HIV disease has been associated with loss of memory T cell responses to antigen. To better characterize and quantify long-lived memory T cells *in vivo*, we have refined an *in vivo* labeling technique to study the kinetics of phenotypically distinct, low frequency $CD8^+$ T cell subpopulations in humans. HIV-negative subjects and antiretroviral-untreated HIV-infected subjects in varying stages of HIV disease were studied. After labeling the DNA of dividing cells with deuterated water (^2H_2O), ^2H-label incorporation and die-away kinetics were quantified using a highly sensitive FACS/mass spectrometric method. Two different populations of long-lived memory $CD8^+$ T cells were identified in HIV-negative subjects: $CD8^+CD45RA^-CCR7^+CD28^+$ central memory (T_{CM}) cells expressing IL-7Rα and $CD8^+CD45RA^+CCR7^-CD28^-$ RA effector memory (T_{Emra}) cells expressing CD57. In pilot studies in HIV-infected subjects, T_{Cm} cells were found to have a shorter half-life and reduced abundance, particularly in those with high viral loads; T_{Emra} cells, by contrast, retained a long half-life and accumulated in the face of progressive HIV disease. These data are consistent with the hypothesis that IL-7Rα$^+$ T_{Cm} cells represent "true" memory $CD8^+$ T cells, the loss of which may be responsible in part for the progressive loss of T cell memory function during progressive HIV infection.

Keywords

Human; T cells; AIDS; Cell proliferation; Memory

[1]This work was supported in part by NIH grant RO1 AI43866 to MKH and NIH awards U01 AI43641 and R37 AI40312 to JMM, who is the recipient of the Burroughs Wellcome Fund Clinical Scientist Award in Translational Research and the NIH Director's Pioneer Award Program, part of the NIH Roadmap for Medical Research, through grant number DPI OD00329. Funding for the optimization of the low-count techniques was provided by KineMed. The Clinical and Translational Science Institute Clinical Research Center (CCRC) was supported by UL1 RR024131-01 from the National Center for Research Resources (NCRR), a component of the National Institutes of Health (NIH), and NIH Roadmap for Medical Research.

2 Address for correspondence: Joseph. M. McCune, M.D., Ph.D., Division of Experimental Medicine, Department of Medicine, University of California San Francisco, 1001 Potrero Ave., Bldg. 3, Rm 601, San Francisco, CA, 94110 Phone 415-206-8101; FAX 415-206-8091; e-mail mike.mccune@ucsf.edu.

†Current address: Department of Medical Biochemistry and Immunology, School of Medicine, Cardiff University, UK

¶Current address: Department of Medicine, University of Cambridge, UK

Introduction

Ever since the onset of the AIDS epidemic, it has been clear that HIV infection is associated with immunodeficiency (1,2). In the intervening years, a number of mechanisms underlying this state of immunodeficiency have been described, ranging form quantitative loss of $CD4^+$ T cells to qualitative changes in cell populations that persist (3,4). Amongst the qualitative changes, one of the earliest to be discerned was the loss of recall response to antigen (5). Such recall, or "memory," responses represent the bedrock upon which the adaptive immune system is based (6-10). In the T cell lineage, memory is associated with specialized cell subpopulations that differentiate from naïve T cells after exposure to antigen. Each memory T cell clone is endowed with an antigen-specific receptor, with the ability to persist for long periods of time, and with the propensity to rapidly proliferate and to differentiate into effector cells after secondary contact with cognate antigen. By this sequence of events, durable antigen-specific immunity is achieved.

Studies carried out in well-defined murine systems have illuminated some of the requirements for generation and maintenance of a memory $CD8^+$ T cell response during and after acute infection (10). Gene expression profiling and functional characterization of murine $CD8^+$ T cell development have demonstrated that $CD8^+$ T cell differentiation proceeds through a series of discrete steps (6,11,12). In mice, long-lived memory $CD8^+$ T cells are thought to originate from effector $CD8^+$ T cells that survive a death phase that follows the initial phase of T cell activation and expansion (13). Requirements for generation and maintenance of such memory $CD8^+$ T cells include $CD4^+$ T cell help (6,14,15) as well as acquisition of the cellular machinery that provides for either self-renewal (e.g., through the action of the transcriptional repressor, bcl6b, which in turn may be important for asymmetric differentiation of antigen-specific T cells upon secondary antigenic challenge) or for limited homeostatic proliferation (e.g., mediated by IL-7 through the IL-7Rα) (6,16,17). Homeostatic renewal itself appears to be dependent upon "rest" from antigenic stimulation, an opportunity less frequent during the course of chronic viral infections that are associated with continuously high viral loads. At the same time, low level persistence of antigen and continued proliferation are likely necessary for the maintenance of virus-specific memory T cells in chronic infection, since these cells are not maintained by homeostatic cytokines (e.g., IL-7 and IL-15), inflammatory signals, and priming of recent thymic emigrants alone (18).

In humans, the long-lived memory $CD8^+$ T cell compartment is poorly understood. Initial studies described three $CD8^+$ T cell subpopulations (naïve, memory, and effector), distinguished by their cell surface phenotype (19). Memory T cells were found to exhibit high proliferative capacity while effector T cells demonstrated strong cytotoxic potential. More recently, based on the presence or absence of expression of the chemokine receptor, CCR7, the memory compartment has been subdivided into "central memory" and "effector memory" subpopulations (20). Since then, additional cell surface markers have been used to distinguish various T cell subpopulations, but different studies have been non-uniform in the use of these markers (21,22). The general consensus is that long-lived memory $CD8^+$ T cells reside within a $CD3^+CD8^+CD45RA^-CD28^+CCR7^+$ central memory T (T_{Cm}) cell population that is endowed with high proliferative capacity, a broad T cell receptor repertoire, and expression of IL-7Rα (19,23). Another subpopulation of $CD8^+$ T cells that may be long-lived *in vivo* (24) is the $CD3^+CD8^+CD45RA^+CD28^-CCR7^-$RA effector memory ($T_{Emra}$) subpopulation. A very high fraction of these cells expresses CD57, a marker associated with senescent T cells (25,26), and it is not clear if they possess substantial memory function *in vivo*.

The fate of these long-lived $CD8^+$ T cell subpopulations is even less well studied in the context of HIV-infected individuals. Usually, HIV disease progression is associated with a decrease in the absolute number of circulating naïve $CD8^+$ T cells (T_N) and an increase in the number

of circulating memory/effector $CD8^+$ T cells. Labeling studies with deuterated glucose or water have shown that the latter compartment can be subdivided into two kinetically distinct subpopulations, one of which is short-lived (presumably containing effector, or T_E, $CD8^+$ T cells) and the other longer-lived (presumably containing the T_{CM} and/or T_{EMRA} cells). In HIV-infected individuals classified as long-term non-progressors, cells with a T_{CM}-like phenotype are maintained in the circulation (27). Antigen-specific $CD8^+$ T_{EMRA} cells are also more frequent in those who control HIV replication after acute infection than in those who develop progressive disease (28). Analytic limitations (e.g., cell numbers below detection limits and low isotope enrichments), however, have made it difficult to directly measure the lifespan of these two cell subpopulations. Accordingly, it is not clear whether their lifespan or relative abundance changes as a function of HIV disease progression.

In this study, we have refined the stable isotope/FACS/mass spectrometric (MS) method for the analysis of T cell turnover *in vivo* so that it can be used to simultaneously measure the *in vivo* kinetics and lifespan of multiple subpopulations of $CD8^+$ T cells, including, for the first time, those that are relatively rare. A long-term (7 week) ^2H_2O labeling protocol was employed, during which time ^2H was incorporated into the deoxyribose moiety of DNA in slowly dividing cells and various $CD8^+$ T cell subpopulations, which were thereafter sort-purified according to their expression of CD45RA, CCR7, and CD28 (21,29-32). Label incorporation and die-away kinetics into each of these subpopulations were then quantified by mass spectrometric analysis (33-37). In addition to evaluating the applicability of the refined stable isotope/FACS/MS to the kinetic analysis of low abundance T cell subpopulations *in vivo*, our aim was to provide information about the following questions: (i) what is the phenotype and the lifespan of long-lived memory $CD8^+$ T cells in healthy HIV-negative subjects, and (ii) does this phenotype and/or lifespan change in the context of progressive HIV disease? Our results demonstrate that the turnover of low abundance T cell subpopulations can be quantified using the refined stable isotope/FACS/MS method. Moreover, data obtained by this method suggest that both $CD8^+$ T_{CM} and T_{EMRA} are long-lived *in vivo* in humans, but that T_{CM} cells are lost and T_{EMRA} cells accumulate as HIV disease progresses.

Materials and Methods

Human subjects

Subjects were recruited by advertisement. Written informed consent was obtained from all subjects and protocols were approved by the University of California at San Francisco Committee on Human Research. Eight HIV-negative and five antiretroviral-untreated HIV-infected subjects were included in the *in vivo* stable isotope labeling study. Except for one subject, all of the labeled HIV-infected subjects were naïve to antiretroviral treatment. All of the labeled subjects were male. Additional immunophenotyping was carried out on four of the labeled and two additional HIV-negative subjects, all five of the labeled HIV-infected subjects, two more HIV-negative subjects (one female and one male), and 15 more chronically infected, antiretroviral-untreated HIV-infected subjects (13 males and two transgender, one of the latter known to be treated with feminizing sex hormones) from the “SCOPE cohort” (an ongoing prospective cohort study aimed at investigating the long-term clinical and immunological consequences associated with HIV infection and treatment of HIV infection) (38). Subjects were excluded if, at any time within the three month period before enrollment, they had either used a medication (e.g., glucocorticoids or other immunosuppressive drugs) or been diagnosed with a disease (e.g., lymphoproliferative diseases or cancer) that might affect T cell turnover. All the labeled subjects came in for a screening visit, at which time they had to fill out a questionnaire and blood was drawn to determine their eligibility to participate in the study. The characteristics of those subjects who were studied are shown in Table I. Changes in the relative proportion of $CD8^+$ T cell subpopulations were discerned by obtaining a complete

blood count and a T cell phenotyping flow cytometric panel (see below) at each sort date. Both $CD8^+$ T cell counts and the relative composition of $CD8^+$ T cell subpopulations were found to be stable for individual subjects during the time period of study.

Labeling protocol

All subjects enrolled for labeling were seen at the Clinical and Translational Science Institute Clinical Research Center (CCRC) at San Francisco General Hospital. After enrollment, they were provided with a sufficient number of 50 ml vials of 70% ^2H_2O (Cambridge Isotope Laboratories Inc., Andover, MA, USA) for a seven-week labeling protocol. During the first week of labeling, subjects drank three vials of 50 ml 70% ^2H_2O per day followed by either two weeks or six weeks of two vials of 50 ml 70% ^2H_2O per day. The first blood draw for cell sorting (Sort 1, or S1) was obtained in most cases three weeks after the last dose of ^2H_2O was taken by the subject (i.e., week 10 after the start of labeling). This blood draw was followed by two further blood draws (i.e., at weeks 14 and 18, termed S2 and S3, respectively). Some subjects came in for an additional blood draw during the last week of labeling (data not shown). This time line is shown in Figure 1A. A pilot study in four healthy subjects labeled for only three weeks with ^2H_2O revealed that ^2H-label incorporation into DNA of the T cells studied was insufficient to characterize die-away curves optimally (data not shown). The longer, seven-week labeling protocol achieved higher initial levels of label incorporation and was therefore used for the data reported here.

Measurement of T cell DNA labeling

The stable isotope/FACS/MS method for measuring T cell turnover has been described in detail previously (33,36,39). This method was refined so that smaller numbers of cells could be analyzed while maintaining accuracy for isotope enrichment (40), enabling the simultaneous kinetic characterization of multiple subpopulations of $CD8^+$ T cells, including rare phenotypic subsets. Briefly, all reagents and buffers were handled with nitrile gloves in a dedicated workspace and were kept scrupulously clean. All kits and reagents were set aside for use with small cell samples and batch tested for contamination of reagents with extraneous deoxyribose or DNA. Sorted cell pellets were resuspended in 200 ml PBS, boiled for 10 min to release DNA from chromatin, and rapidly chilled. For DNA hydrolysis, 50 ml 5× concentrated hydrolysis cocktail was added, containing sodium acetate buffer, pH 5, zinc sulfate, nuclease S1, and acid phosphatase (41), and the mixture was incubated at 37 °C for 1-16 hours. Samples were transferred to 16 mm × 100 mm screw-capped glass hydrolysis tubes. Aqueous O-(2,3,4,5,6-pentafluorobenzyl)-hydroxylamine hydrochloride (PFBHA) solution (1 mg/ml, 100 μl) was added, followed by 75 μL glacial acetic acid, and the mixtures incubated at 100°C for 30 min. After cooling to room temperature, 1 mL of acetic anhydride was added to each sample, followed by 100 μL of N-methylimidazole with rapid mixing. The reaction was allowed to proceed for 15-20 min. After cooling, two mL water were added, and the reactions were extracted twice with 750 μL dichloromethane. The organic layers were pooled, dried over sodium sulphate, evaporated to dryness, reconstituted in 50 ml ethyl acetate, and transferred to gas chromatography (GC) vials for analysis.

In addition to controls employed routinely in the stable isotope/FACS/MS method (33,36, 39), additional sets of blanks and standards were included in each run. DNA standards were approximately matched to the range of cell counts in the experimental samples, assuming about 6 pg DNA per human diploid nucleus. Labeled cell samples and DNA standards of known ^2H enrichment were diluted and run with each preparation to verify the stability of measured enrichments at low sample abundance, and reagent blanks were used to assess contamination by extraneous deoxyribose or DNA. Before analyzing samples with low cell counts, the entire procedure was checked several times, using only DNA standards, blanks, and titrated amounts of cells from an abundant source with known ^2H enrichment.

Gas chromatographic (GC)/MS analysis was performed using an Agilent (Palo Alto, California, USA) model 5973 MS with a 6890 GC and an autosampler in negative chemical ionization mode with methane as reagent gas. Samples were resolved on a 30-m DB-17 column with helium as the carrier gas, and selected ion monitoring was used to quantify the fractional molar abundances of the parent ion [M − HF, = M0] *(m/z* 435) and the M1 mass isotopomer *(m/z* 436) of the pentafluoro tri-acetate (PFTA) derivative of dR. ^{2}H enrichment was calculated as EM1, the excess fractional abundance of the M1 mass isotopomer above baseline (as determined by analysis of the unlabeled deoxyribose derivative, with correction for analyte abundance effects) (39). The EM1 value represents isotope enrichment from ^{2}H above natural abundance and is analogous to specific activity values with radioisotopes (33,42). Data were rejected if the signal to background ratio fell below 10, or if the M0 abundance fell below the abundance range that generated reliable EM1 values with the diluted, labeled standards. ^2H_2O enrichments in body water were calculated as described previously (34,39) by comparison to standard curves generated by mixing 100% ^2H_2O with natural abundance H_2O in known proportions.

Preparation of whole blood samples for sorting

Fresh peripheral blood mononuclear cells (PBMC) (on average, 1×10^8 and 1.7×10^8 PBMC from 80 ml of blood from HIV-negative or HIV-infected subjects, respectively) were obtained by density centrifugation using Ficoll-Hypaque (Sigma-Aldrich, St. Louis, MO, USA) and stained using the following antibodies purchased from BD Pharmingen (BD Pharmingen, San Jose, CA, USA): anti-CD3-Alexa700, anti-CD8-Pacific Blue, anti-CCR7-PE-Cy7, anti-CD28-APC, anti-IL-7 receptor(R)-PE, and anti-CD57-FITC. Additional antibodies used for staining were anti-CD45RA-ECD (Beckman Coulter, Fullerton, CA, USA), anti-IL-18R1α-FITC (Serotec Inc., Raleigh, NC, USA), and anti-CD27-APC-Cy7 or -Alexa750 (eBioscience, San Diego, CA, USA). Live/dead® fixable aqua (Amine) (Invitrogen Corporation, Carlsbad, California, USA) was used for T cell phenotyping of an additional 15 HIV-infected subjects and two HIV-negative subjects that were not labeled with ^2H_2O. $CD3^+CD8^+$ T cell subpopulations (comprising at least one sample of 20,000 cells of each subpopulation and duplicates to quadruplicates of 10,000-100,000 cells, if possible) were sorted on a triple-laser BD FACS Digital Vantage or a quadruple-laser BD FACS Aria (both from Becton Dickinson Immunocytometry Systems, San Jose, CA, USA), based on the presence or absence of CD45, CCR7, CD28, and/or CD57 expression. Gates for the T cell subpopulations were set based on fluorescence minus one (FMO) stained PBMC ($0.6 - 1.2 \times 10^6$ cells stained in 100 μl). The sort samples were stained with only the following antibodies: anti-CD3, anti-CD8, anti-CD45RA, anti-CCR7, anti-CD28, and anti-CD57.

Calculations of decay constants, half-lives, and percentage of $CD8^+$ T cells remaining after 7 weeks of ^2H_2O labeling

As in previous studies (33,39), ^2H_2O kinetic calculations during the ^{2}H-label incorporation phase were based on the precursor-product relationship. In this pulse/chase experiment, the loss of label enrichment in cellular DNA during the de-labeling phase was determined for each T cell subset. ^{2}H enrichment in cellular DNA at S1 (week 10, or three weeks after the last dose of ^2H_2O), representing the baseline value (or pulse) after wash-out of ^2H_2O from body water pools, was used as the time zero value. This time point was chosen because body water ^2H_2O enrichments fall to low levels (i.e., with a half-life of approximately 7 days, data not shown), allowing subsequent die-away kinetics to be assessed without the confounding effects of continued label incorporation. The subsequent loss of label from cellular DNA of each subset was quantified between S1 and S3 (week 18). The decay constant (k) was calculated using the equation for exponential decay: $k = -[\ln(S3/S1)]/Dt$, where S3 and S1 represent ^{2}H enrichments measured at weeks 18 and 10, respectively, and Dt is the time between measurements (8 weeks). The half-life was calculated as $t_{1/2} = \ln(2)/k$. For some T cell subpopulations in some

individuals (e.g., T_N cells in subjects, who were HIV-negative), exponential label decay was not observed between S1 and S3. Therefore, we also calculated the percentage of initially incorporated label (i.e., the ^2H enrichment measured at S1) that was retained at S3 (i.e., percent labeled cells remaining = [S3/S1]). This parameter does not assume any particular kinetic model of cell survival, such as a single-pool, single-exponential kinetics of label die-away and was calculated for all cell populations.

Statistical analyses

Statistically significant differences between groups were assessed using the parametric Student's t test. The parametric Pearson correlation (calculated with 95% confidence intervals and two-tailed p values) was used to determine the strength of linear relationships between two variables. Parametric statistical tests were applied due to their greater sensitivity with the low sample sizes found in some of the analyses of this study. All data sets were tested for normality using the Kolmogorov-Smirnov normality test and all that showed significant differences were found to be normal using this test.

Results

Characteristics of study populations

To investigate the impact of HIV infection on long-lived $CD8^+$ T cell subpopulations, we first phenotypically characterized the $CD8^+$ T cell compartment in antiretroviral-untreated HIV-infected subjects at varying stages of disease (n = 20, including five labeled HIV-infected subjects) and compared the results to those obtained in healthy HIV-negative subjects (n = 6, comprising four subjects labeled with ^2H_2O and two additional subjects who were not labeled). Long-term (seven week) *in vivo* ^2H_2O labeling was also carried out in five of the HIV-infected subjects and four of the HIV-negative subjects. The median CD8 count of the HIV-infected subjects (1175 CD8 T cells/μl; range 578-3388) was significantly higher than that of the HIV-negative subjects (334 CD8 T cells/μl; range 246 – 563) ($p<0.002$ HIV-infected versus HIV-negative). This fact, coupled with refinements made to the FACS/MS method for measurements with low cell numbers enabled the analysis of more $CD8^+$ T cell subpopulations from HIV-infected than from HIV-negative subjects. Further characteristics of the study subjects are shown in Table I and the time line of the labeling protocol is shown in Figure 1A.

With progressive HIV disease, the number of circulating T_N and T_{CM} cells decreases while the number of T_{EMRA} cells remains high

The cell surface markers used to differentiate effector memory (T_{EM}), effector T (T_E), RA effector memory T (T_{EMRA}), central memory T (T_{CM}), or naïve T (T_N) cell subpopulations within the $CD3^+CD8^+$ population were chosen based on findings from previous human studies (21,29-32). The gating strategy used for cell sorting and analysis is shown in Figure 1B. The cytometric flow profiles in Figures 2 and 3 show the different $CD3^+CD8^+$ T cell subpopulations studied here, including $CD45RA^{bright}CCR7^+CD28^+$ (T_N), $CD45RA^{bright}CCR7^-CD28^-$ (T_{EMRA}), $CD45RA^-CCR7^+CD28^+$ (T_{CM}), and $CD45RA^-CCR7^-CD28^-$ (T_E) cells from five HIV-negative subjects and 20 HIV-infected subjects with a range of CD4 counts, sorted by decreasing CD4 counts. It is evident from the flow cytometric profiles shown in Figure 3 that the $CD8^+CD45RA^-CCR7^-$ T cells, which are here referred to as T_{EM} cells (red box), are heterogeneous and consist of two distinct subpopulations when analyzed for expression of CD45RA, CCR7, and CD28, namely $CD45RA^-CCR7^-CD28^+$ and $CD45RA^-CCR7^-CD28^-$ cells (red box around T_{EM} cells in Figure 3A, right flow plot in the upper row).

The relationship of each of these $CD3^+CD8^+$ T cell subpopulations to the CD4 count was assessed in the cohort of HIV-infected subjects (Figure 4). As shown in Figure 4A, the absolute number of $CD3^+CD8^+$ T cells remained more or less constant across the range of CD4 T cell

counts studied in this cohort. It has been previously reported that the transition of HIV-specific cells from the T_{EM} phenotype to the T_{EMRA} phenotype does not occur (43,44). In line with this finding, the fraction of total T_{EM} cells is increased in most HIV-infected subjects as compared to HIV-negative subjects (median 69.6%, IQR 44.5% – 82.6% T_{EM} cells in HIV-infected subjects versus median 9.9%, IQR 5.6% – 19.3% T_{EM} cells in HIV-negative subjects, $p<0.0001$). There was no significant correlation between T_{EM} cells per μl of blood and the CD4 count in HIV-infected subjects (Figure 4B). Similarly, although the flow cytometric profiles reveal an increase in the fraction of T_E cells in some HIV-infected subjects as compared to most HIV-negative subjects (median 6.5% IQR 3% – 11% T_E cells in HIV-infected subjects versus median 1.6% IQR 0.6% – 3.2% T_E cells in HIV-negative subjects, $p=0.08$), there was no significant correlation between the absolute number of T_E $CD8^+$ T cells and the CD4 count (Figure 4C). Moreover, $CD8^+$ T cells with a T_{EMRA} phenotype were rare in healthy HIV-negative subjects (see Figure 2A), but their fraction and absolute number was elevated in HIV-infected subjects, irrespective of the CD4 count (median 273 [21.4%] IQR 182 – 406 [16% – 28%] T_{EMRA} cells in HIV-infected subjects versus median 22 [7.2%] IQR 19 – 39 [4% – 12%] T_{EMRA} cells in HIV-negative subjects, $p<0.01$), even though there was no relationship between their absolute count and the CD4 count (Figure 4D). In contrast, the number of T_{CM} cells was observed to fall as the CD4 count declined ($p=0.02$) (Figure 4E). Finally, and consistent with the previously reported decrease of T_N cell numbers found in adults with progressive HIV disease (45), T_N cells significantly decreased with decreasing CD4 counts ($p=0.02$) (Figure 4F).

In HIV infection, T_{EMRA} cells maintain a long lifespan but T_{CM} cells do not

The seven-week ^2H_2O labeling protocol resulted in higher ^2H_2O enrichments in the different T cell subpopulations of HIV-negative subjects, including long-lived T_N cells, than did three weeks of ^2H_2O labeling (data not shown). This finding is consistent with a meta-analysis of previous stable isotope labeling studies with different periods of labeling, which showed that longer labeling protocols resulted in progressive incorporation of label into longer-lived cells (46).

$CD3^+CD8^+$ T cells ("$CD8^+$ T cells"), T_{EM}, T_E, T_{EMRA}, T_{CM}, and T_N cells from HIV-negative and HIV-infected subjects were sorted and analyzed for ^2H_2O label enrichment after 7 weeks of ^2H_2O labeling and during the subsequent de-labeling period. Figure 5 shows the decay curves of label enrichment in each of these subpopulations. A few points are apparent. First, the observation of consistent and distinct patterns of label enrichment in the different T cell subpopulations confirms that use of the refined stable isotope/FACS/MS method allowed measurement of label incorporation into as few as 5,000 - 20,000 cells (the data shown here were generally derived from 20,000 cells). Secondly, it is evident from the labeling patterns that HIV-infected subjects had higher levels of label enrichment in several T cell subpopulations studied than HIV-negative subjects, as would have been expected from previous studies (34,39). Also, label incorporation into T_{EM} cells from HIV-negative subjects was relatively high, but varied between subjects at the different time points (Figure 5C), possibly reflecting their heterogeneous phenotypic composition in these HIV-negative subjects (Figure 3A). In HIV-infected subjects, label incorporation into the T_{EM} subpopulation was higher, especially in the HIV-infected subject with the highest VL (open squares in Figure 5D).

Additional insights into the turnover of different $CD8^+$ T cell subpopulations were obtained upon inspection of the die-away curves. In the case of the T_E subpopulation, a high fraction of these cells was labeled in four HIV-infected subjects, and a rapid de-labeling occurred during the period of observation (Figure 5E). Given the small numbers of such cells in HIV-negative subjects, the kinetics of this subpopulation could only be studied in a single individual (filled symbols in Figure 5E). Label incorporation and rapid loss of label in T_{EM} cells of HIV-infected

subjects was very similar to that of T_E cells, notwithstanding the heterogeneous composition of the former subpopulation. In HIV-negative subjects, the T_{EMRA} (Figure 5F) and T_{CM} (Figure 5G) subpopulations both revealed low uptake of label and slow loss after labeling was discontinued. In all HIV-infected subjects, T_{EMRA} cells also showed a very slow loss of label (Figure 5F). In contrast, however, some but not all HIV-infected subjects showed a high uptake of label and a very rapid loss of label in the T_{CM} subpopulation (Figure 5H). Label incorporation into T_N cells was low in both HIV-negative and HIV-infected subjects (on average 0.18% in HIV-negative subjects versus 0.4% in HIV-infected subjects) and its loss after cessation of labeling was slow, if evident at all in HIV-negative subjects, consistent with the expected long half-life of this subpopulation of cells (9, 34) (Figure 5I, 5J). Label decreased or was lost completely by the last time point in T_N cells from HIV-infected subjects with high VLs, however.

The decay curves shown in Figure 5 were used to calculate the decay constant (k) and the half-life as well as the percentage of cells remaining at the end of the labeling period. These data are summarized in Table II, along with the number of cells per μl and the frequency of a given subpopulation among total $CD8^+$ T cells. T_{EM} cells had a very variable half-life (mean 105.8 ± 88.4 days) in HIV-negative subjects, likely due to the fact that the fraction of $CD28^+$ and $CD28^-$ cells within this $CD8^+$ T cell subpopulation was variable in these subjects. This variability was also reflected in the variable percentage of T_{EM} cells remaining at week 18. In HIV-infected subjects, in contrast, the half-life of T_{EM} cells was shorter and less variable (35.9 +/- 4.1 days) and the percentage of cells remaining at week 18 was similar to that found for T_E cells. T_E cells, meanwhile, showed a short half-life in both HIV-negative and HIV-infected subjects (58.1 and 49.3 (+/- 19.3) days, respectively). Of the memory/effector $CD8^+$ T cell subpopulations, T_{EMRA} and T_{CM} cells had the longest half-lives (9762 and 97.7 days, respectively) in the HIV-negative subjects and also the highest fraction of cells (99.6% and 64.9%, respectively) remaining at the last time point evaluated during de-labeling. However, while T_{EMRA} cells in HIV-infected subjects had a long half-life irrespective of the VL, the half-life of T_{CM} cells was shorter (51 days) and was particularly short (28.8 days) in those with a high VL ($p<0.05$). In those subjects with a high VL, the fraction of remaining labeled T_{CM} cells was significantly reduced at the end of the labeling period (26.0% versus 74.7% in those with a low VL and versus 64.9% in HIV-negative subjects; $p<0.01$ for HIV-negative subjects versus HIV-infected subjects with high VL). By contrast, the fraction of T_{EMRA} cells remaining at the end of the labeling period was the same (68.5% ± 10.6%), irrespective of the VL. Although the half-life of cells in the T_N cell compartment could not be estimated (see Table II legend), the percentage of labeled T_N cells remaining at the end of the de-labeling period was significantly lower in HIV-infected subjects than in HIV-negative subjects (42.8% versus 175.5%, $p<0.01$). Of note, the subject with the highest VL had the lowest number of T_N cells (range 23-66 T_N cells per μl at three different sort days), consistent with the trend observed (Figure 4E, ref. 24) between loss of T_N cells and progressive HIV disease.

More detailed correlations between HIV VL and the percentage of T_{Em}, T_e, T_{Emra}, or T_{Cm} cells remaining are shown in Figure 6. No clear trend was observed for the correlation between VL and T_{Em} cells remaining (Figure 6A), likely due to their heterogeneous phenotypic composition. The more homogenous subpopulation of remaining T_E cells, however, significantly correlated negatively with VL ($p<0.01$) (Figure 6B). There was no significant correlation of VL and the percentage of T_{EMra} cells remaining (Figure 6C), but a significant correlation was found between VL and the percentage of T_{Cm} cells remaining at the last time point during de-labeling ($p<0.05$) (Figure 6D). These observations are consistent with the decline in T_{Cm} cells observed with decreasing CD4 counts documented in the larger cohort of HIV-infected subjects (Figure 4D).

Expression of IL-7Rα, IL-18R1α, and CD57 on T_{Cm} and T_{Emra} cells in the different $CD8^+$ T cell subpopulations

Because long-lived memory T cells may behave like self-renewing stem cells (16,17,47), we asked whether long-lived T_{Cm} cells or T_{EMra} cells express certain cell surface receptors (e.g., IL-7Rα and IL-18R1α) that have been previously shown (16) to be expressed on murine hematopoietic stem cells as well as on memory B and T cells. We also evaluated changes in the expression patterns of these surface receptors between HIV-negative and HIV-infected subjects in varying stages of disease progression as well as the fraction expressing CD57, a marker of more terminally differentiated cells. As shown in Figure 7A (left), almost 100% of T_{Cm} cells from healthy HIV-negative subjects express IL-7Rα, while the percentage of IL-7Rα$^+$ T_{Cm} cells was significantly lower in HIV-infected subjects ($p<0.05$). Expression of IL-18R1α or CD57 on T_{Cm} cells was much lower and did not differ between groups. The fraction of T_{Emra} cells expressing IL-7Rα was significantly lower in HIV-infected subjects than in HIV-negative subjects ($p<0.01$) (Figure 7B, left) as was the fraction expressing IL-18R1α ($p<0.05$) (Figure 7B, middle) and CD57 ($p<0.05$) (Figure 7B, right). When these subpopulations were examined in the context of CD4 T cell counts, the percentage of T_{Cm} cells positive for IL-7Rα trended to fall as the CD4 count fell (Figure 7C, left). There was a significant decrease in the MFI of CD57 on $CD8^+$ T cells and this decrease was specifically observed on $CD8^{high}$ T_{Emra} cells ($p=0.003$) (Figure 7C, middle) and a decrease in the percentage of $CD8^{high}$ T_{Emra} cells that were $CD57^+$ ($p=0.06$) (Figure 7C, right).

Discussion

It is clear that the memory/effector $CD8^+$ T cell population is phenotypically and functionally heterogeneous, including multiple subpopulations of short-lived effector cells and long-lived memory cells (39,48). In a previous study using an *in vivo* labeling technique (34), we found that long-lived $CD4^+$ and $CD8^+$ T cell subpopulations are lost as a function of HIV disease progression. Here, we have used a refinement of this labeling technique that permitted kinetic characterization of the lifespan of small numbers of cells to discern two subpopulations of long-lived $CD8^+$ T memory/effector cells: $CD8^+CD45RA^-CCR7^+CD28^+$ central memory (T_{Cm}) cells expressing IL-7Rα and $CD8^+CD45RA^+CCR7^-CD28^-$ RA effector memory (T_{Emra}) cells, of which a high fraction expresses CD57. Especially in HIV-infected subjects compared to healthy HIV-negative subjects, T_{Cm} cells were found to have a significantly shorter half-life in HIV-infected subjects with high viral loads, compared to healthy HIV-negative subjects, and to decrease in number and in their expression of IL-7Rα as a function of disease progression. T_{Emra} cells, by contrast, retained a long half-life, accumulated in the face of progressive HIV disease, and lost expression of CD57. These observations reveal kinetic differences between certain subpopulations of $CD8^+$ T cells in HIV-infected subjects that may be related to disease progression.

An important, and we believe generally applicable, feature of this study is its demonstration that the kinetics of thousands, as opposed to hundreds of thousands, of cells can be studied *in vivo*. Prior methodology could only be used to estimate the half-life of larger numbers of cells that were assumed to contain varying fractions of phenotypically distinct subpopulations. By using the newly refined techniques described here for accurate measurement of isotope enrichments in small numbers of cells, combined with the use of long-term “pulse” labeling with ^2H_2O, it is now possible to take full advantage of the power of state-of-the-art multiparameter, multidirectional fluorescence-activated cell sorting and to simultaneously measure the kinetics of multiple, even rare, subpopulations of cells. A caveat to any interpretation that might be drawn from our kinetic analysis is that the number of subjects studied (4 HIV-negative and 5 HIV-infected) is small. Nonetheless, and especially when

coupled with phenotypic data obtained from an additional 17 subjects, a number of conclusions can be reasonably drawn.

First, the $CD8^+$ T_{Cm} subpopulation that we show to be long-lived ($t_{1/2}$ = 97.7 days) in HIV-negative subjects has die-away kinetics that are markedly faster in HIV-infected subjects, with a half-life reaching 28.8 days in those with the highest viral loads. Concomitantly, this subpopulation is lost from the circulation as the CD4 count drops with disease progression. Possibly, T_{Cm} cells are lost because they are less efficiently produced: circulating naïve $CD8^+$ T cell progenitors to these cells decline in number as a function of HIV disease progression (45). Alternatively or in addition, T_{Cm} cells may be lost because they survive less well. Thus, while IL-7 is necessary for the survival of long-lived memory T cells (49), the high levels of IL-7 (50,51) and of chronic immune activation (38,52) found in late-stage HIV disease may result in down-regulation of the IL-7Rα on T_{Cm} cells, as reported previously (53-58) and as also observed in these studies. Such down-regulation, in turn, would have predictably negative impact on T_{Cm} cell survival (59). In addition, T_{Cm} cells could transition more rapidly and/or in larger numbers to shorter-lived T_E cells in HIV-infected individuals, similar to the observation made recently in SIV-infected macaques (60). It is also possible that maintenance of the $CD8^+$ T_{Cm} compartment is dependent upon preservation of $CD4^+$ T_{Cm} cells, which have been shown to be lost as a function of progressive SIV disease (60) and are likely also lost in progressive HIV disease (34).

A second tentative conclusion is underscored by the markedly different behavior of the long-lived T_{Emra} subpopulation. In HIV-negative subjects, these cells are low in number and slow in turnover. By contrast, circulating numbers of T_{Emra} cells are generally much higher in HIV-infected subjects, in whom they are also found to lose the expression of CD57, IL-7Rα, and IL-18R1α, but to remain long-lived. Collectively, these observations suggest that T_{Emra} cells maintain a long lifespan in HIV-infected subjects but that they change phenotypically, and perhaps also functionally, as HIV disease progresses. Thus, it has recently been shown that HIV-specific T_{Emra} cells in early infection are linked to control of HIV viremia and predict the subsequent VL set point (61); in this stage of disease and with this phenotype, they may be protective. Reciprocally, the $CD57^{low}$ T_{Emra} cells that accumulate in late stage disease may not share the same properties and may not be beneficial.

In the present study, we also addressed the question of whether cells in either of the long-lived memory $CD8^+$ T cell subpopulations have properties similar to those of stem cells. In previous studies, for example, it has been proposed that bcl6b is responsible for maintaining “stem cell-like” memory T cells in a quiescent state (17,29) and, by microarray analysis, transcripts for IL-7Rα and IL-18R1α have been detected within murine hematopoietic stem cells, memory B cells, and memory T cells (16). In our hands, the expression of bcl6b was not higher in memory than in naïve T cells (data not shown) and T_{Cm} cells were found to express IL-7Rα but only a small fraction (approximately 20%) expressed IL-18R1α. Thus, at this level of discrimination, we are unable to ascribe accepted traits of stem cells to these human $CD8^+$ memory T cell subpopulations.

In summary, a highly sensitive *in vivo* labeling technique has been used here to define the kinetic properties of low abundance subpopulations of $CD8^+$ T cells, including T_{EM}, T_{EMRA}, T_E, T_{CM}, and T_N cells, in healthy subjects as well as in those infected with HIV. The data show that long-lived $CD8^+$ T cell subpopulations in healthy human subjects include T_N, T_{CM}, and T_{EMRA} cells. In progressive HIV infection, the half-life of T_{CM} cells becomes shorter while that of T_{EMRA} cells remains the same. These changes in kinetics are reflected in the composition of the total $CD8^+$ T cell pool: progressive disease is associated with a loss of T_{CM} cells while the fraction and absolute number of T_{EMRA} cells is increased, irrespective of disease stage. Further exploration of these observations using the refined stable isotope/FACS/MS method

may provide a more complete understanding of the manner in which the $CD8^+$ T cell compartment is eroded, both numerically and functionally, as HIV disease advances.

Acknowledgements

We would like to thank the participants of the study, the nurses at the Clinical and Translational Science Institute Clinical Research Center (CCRC) at San Francisco General Hospital, and Rebecca Hoh, Marcia Smith, Joy Madamba, and Regan Gage at the Positive Health Program (PHP), San Francisco General Hospital, San Francisco, CA, USA, for subject selection and recruitment from the SCOPE cohort. We acknowledge Dr. Steven Deeks from the UCSF Positive Health Program (PHP) for his advice on the selection criteria of the subjects from the SCOPE cohort and Dr. Jason Barbour from the PHP for his assistance with the statistical analysis. We appreciate the help with cell sorting by Dr. Marty Bigos, Tomasz Poplonski, and Valerie Stepps from the Flow Cytometry Core at the J. David Gladstone Institutes (San Francisco) and by Ck Poon from the Flow Cytometry Core at the UCSF Division of Experimental Medicine. Lastly, we thank Dr. Claire Emson, Ben Hunrichs, and Bridget McEvoy-Hein of the Department of Nutritional Sciences at UC Berkeley for technical assistance.

Nonstandard abbreviations used

^2H_2O
: deuterated water

T_{CM}
: central memory

T_{EMRA}
: RA effector memory

T_E
: effector

T_N
: naive

WBC
: white blood count differential

GC
: gas chromatographic

MS
: mass spectrometric

S
: sort

NA
: not available

References

1. Evatt BL, Gomperts ED, McDougal JS, Ramsey RB. Coincidental appearance of LAV/HTLV-III antibodies in hemophiliacs and the onset of the AIDS epidemic. N Engl J Med 1985;312:483. [PubMed: 2982095]
2. McCune JM. HIV-1: the infective process in vivo. Cell 1991;64:351. [PubMed: 1988152]
3. Grossman Z, Meier-Schellersheim M, Paul WE, Picker LJ. Pathogenesis of HIV infection: what the virus spares is as important as what it destroys. Nat Med 2006;12:289. [PubMed: 16520776]
4. McCune JM. The dynamics of CD4+ T-cell depletion in HIV disease. Nature 2001;410:974. [PubMed: 11309627]

5. Clerici M, Stocks NI, Zajac RA, Boswell RN, Lucey DR, Via CS, Shearer GM. Detection of three distinct patterns of T helper cell dysfunction in asymptomatic, human immunodeficiency virus-seropositive patients. Independence of CD4+ cell numbers and clinical staging. J Clin Invest 1989;84:1892. [PubMed: 2574188]
6. Kaech SM, Tan JT, Wherry EJ, Konieczny BT, Surh CD, Ahmed R. Selective expression of the interleukin 7 receptor identifies effector CD8 T cells that give rise to long-lived memory cells. Nat Immunol 2003;4:1191. [PubMed: 14625547]
7. Schluns KS, Lefrancois L. Cytokine control of memory T-cell development and survival. Nat Rev Immunol 2003;3:269. [PubMed: 12669018]
8. Seder RA, Ahmed R. Similarities and differences in CD4+ and CD8+ effector and memory T cell generation. Nat Immunol 2003;4:835. [PubMed: 12942084]
9. Tough DF, Sprent J. Life span of naive and memory T cells. Stem Cells 1995;13:242. [PubMed: 7613491]
10. Wherry EJ, Ahmed R. Memory CD8 T-cell differentiation during viral infection. J Virol 2004;78:5535. [PubMed: 15140950]
11. Kaech SM, Hemby S, Kersh E, Ahmed R. Molecular and functional profiling of memory CD8 T cell differentiation. Cell 2002;111:837. [PubMed: 12526810]
12. Wherry EJ, Teichgraber V, Becker TC, Masopust D, Kaech SM, Antia R, von Andrian UH, Ahmed R. Lineage relationship and protective immunity of memory CD8 T cell subsets. Nat Immunol 2003;4:225. [PubMed: 12563257]
13. Kaech SM, Wherry EJ, Ahmed R. Effector and memory T-cell differentiation: implications for vaccine development. Nat Rev Immunol 2002;2:251. [PubMed: 12001996]
14. Sun JC, Williams MA, Bevan MJ. CD4+ T cells are required for the maintenance, not programming, of memory CD8+ T cells after acute infection. Nat Immunol 2004;5:927. [PubMed: 15300249]
15. Janssen EM, Droin NM, Lemmens EE, Pinkoski MJ, Bensinger SJ, Ehst BD, Griffith TS, Green DR, Schoenberger SP. CD4+ T-cell help controls CD8+ T-cell memory via TRAIL-mediated activation-induced cell death. Nature 2005;434:88. [PubMed: 15744305]
16. Luckey CJ, Bhattacharya D, Goldrath AW, Weissman IL, Benoist C, Mathis D. Memory T and memory B cells share a transcriptional program of self-renewal with long-term hematopoietic stem cells. Proc Natl Acad Sci U S A 2006;103:3304. [PubMed: 16492737]
17. Fearon DT, Manders P, Wagner SD. Arrested differentiation, the self-renewing memory lymphocyte, and vaccination. Science 2001;293:248. [PubMed: 11452114]
18. Shin H, Blackburn SD, Blattman JN, Wherry EJ. Viral antigen and extensive division maintain virus-specific CD8 T cells during chronic infection. J Exp Med 2007;204:941. [PubMed: 17420267]
19. Hamann D, Baars PA, Rep MH, Hooibrink B, Kerkhof-Garde SR, Klein MR, van Lier RA. Phenotypic and functional separation of memory and effector human CD8+ T cells. J Exp Med 1997;186:1407. [PubMed: 9348298]
20. Lanzavecchia A, Sallusto F. Progressive differentiation and selection of the fittest in the immune response. Nat Rev Immunol 2002;2:982. [PubMed: 12461571]
21. Appay V, Rowland-Jones SL. Lessons from the study of T-cell differentiation in persistent human virus infection. Semin Immunol 2004;16:205. [PubMed: 15130505]
22. Harari A, Dutoit V, Cellerai C, Bart PA, Du Pasquier RA, Pantaleo G. Functional signatures of protective antiviral T-cell immunity in human virus infections. Immunol Rev 2006;211:236. [PubMed: 16824132]
23. Kim HR, Hong MS, Dan JM, Kang I. Altered IL-7Ralpha expression with aging and the potential implications of IL-7 therapy on CD8+ T-cell immune responses. Blood 2006;107:2855. [PubMed: 16357322]
24. Wallace DL, Zhang Y, Ghattas H, Worth A, Irvine A, Bennett AR, Griffin GE, Beverley PC, Tough DF, Macallan DC. Direct measurement of T cell subset kinetics in vivo in elderly men and women. J Immunol 2004;173:1787. [PubMed: 15265909]
25. Le Priol Y, Puthier D, Lecureuil C, Combadiere C, Debre P, Nguyen C, Combadiere B. High cytotoxic and specific migratory potencies of senescent CD8+ CD57+ cells in HIV-infected and uninfected individuals. J Immunol 2006;177:5145. [PubMed: 17015699]

26. Brenchley JM, Karandikar NJ, Betts MR, Ambrozak DR, Hill BJ, Crotty LE, Casazza JP, Kuruppu J, Migueles SA, Connors M, Roederer M, Douek DC, Koup RA. Expression of CD57 defines replicative senescence and antigen-induced apoptotic death of CD8+ T cells. Blood 2003;101:2711. [PubMed: 12433688]
27. Migueles SA, Laborico AC, Shupert WL, Sabbaghian MS, Rabin R, Hallahan CW, Van Baarle D, Kostense S, Miedema F, McLaughlin M, Ehler L, Metcalf J, Liu S, Connors M. HIV-specific CD8 + T cell proliferation is coupled to perforin expression and is maintained in nonprogressors. Nat Immunol 2002;3:1061. [PubMed: 12368910]
28. Addo MM, Draenert R, Rathod A, Verrill CL, Davis BT, Gandhi RT, Robbins GK, Basgoz NO, Stone DR, Cohen DE, Johnston MN, Flynn T, Wurcel AG, Rosenberg ES, Altfeld M, Walker BD. Fully differentiated HIV-1 specific CD8+ T effector cells are more frequently detectable in controlled than in progressive HIV-1 infection. PLoS ONE 2007;2:e321. [PubMed: 17389912]
29. Manders PM, Hunter PJ, Telaranta AI, Carr JM, Marshall JL, Carrasco M, Murakami Y, Palmowski MJ, Cerundolo V, Kaech SM, Ahmed R, Fearon DT. BCL6b mediates the enhanced magnitude of the secondary response of memory CD8+ T lymphocytes. Proc Natl Acad Sci U S A 2005;102:7418. [PubMed: 15833813]
30. Sallusto F, Langenkamp A, Geginat J, Lanzavecchia A. Functional subsets of memory T cells identified by CCR7 expression. Curr Top Microbiol Immunol 2000;251:167. [PubMed: 11036772]
31. Michie CA, McLean A, Alcock C, Beverley PC. Lifespan of human lymphocyte subsets defined by CD45 isoforms. Nature 1992;360:264. [PubMed: 1436108]
32. Hamann D, Roos MT, van Lier RA. Faces and phases of human CD8 T-cell development. Immunol Today 1999;20:177. [PubMed: 10203715]
33. Hellerstein M, Hanley MB, Cesar D, Siler S, Papageorgopoulos C, Wieder E, Schmidt D, Hoh R, Neese R, Macallan D, Deeks S, McCune JM. Directly measured kinetics of circulating T lymphocytes in normal and HIV-1-infected humans. Nat Med 1999;5:83. [PubMed: 9883844]
34. Hellerstein MK, Hoh RA, Hanley MB, Cesar D, Lee D, Neese RA, McCune JM. Subpopulations of long-lived and short-lived T cells in advanced HIV-1 infection. J Clin Invest 2003;112:956. [PubMed: 12975480]
35. Macallan DC, Fullerton CA, Neese RA, Haddock K, Park SS, Hellerstein MK. Measurement of cell proliferation by labeling of DNA with stable isotope-labeled glucose: studies in vitro, in animals, and in humans. Proc Natl Acad Sci U S A 1998;95:708. [PubMed: 9435257]
36. Neese RA, Misell LM, Turner S, Chu A, Kim J, Cesar D, Hoh R, Antelo F, Strawford A, McCune JM, Christiansen M, Hellerstein MK. Measurement in vivo of proliferation rates of slow turnover cells by 2H2O labeling of the deoxyribose moiety of DNA. Proc Natl Acad Sci U S A 2002;99:15345. [PubMed: 12424339]
37. Neese RA, Siler SQ, Cesar D, Antelo F, Lee D, Misell L, Patel K, Tehrani S, Shah P, Hellerstein MK. Advances in the stable isotope-mass spectrometric measurement of DNA synthesis and cell proliferation. Anal Biochem 2001;298:189. [PubMed: 11700973]
38. Hunt PW, Martin JN, Sinclair E, Bredt B, Hagos E, Lampiris H, Deeks SG. T cell activation is associated with lower CD4+ T cell gains in human immunodeficiency virus-infected patients with sustained viral suppression during antiretroviral therapy. J Infect Dis 2003;187:1534. [PubMed: 12721933]
39. McCune JM, Hanley MB, Cesar D, Halvorsen R, Hoh R, Schmidt D, Wieder E, Deeks S, Siler S, Neese R, Hellerstein M. Factors influencing T-cell turnover in HIV-1-seropositive patients. J Clin Invest 2000;105:R1. [PubMed: 10712441]
40. Busch R, Neese RA, Awada M, Hayes GM, Hellerstein MK. Measurement of cell proliferation by heavy water labeling. Nat Protocols. 2007In press
41. Busch R, Cesar D, Higuera-Alhino D, Gee T, Hellerstein MK, McCune JM. Isolation of peripheral blood CD4(+) T cells using RosetteSep and MACS for studies of DNA turnover by deuterium labeling. J Immunol Methods 2004;286:97. [PubMed: 15087225]
42. Hellerstein MK, Neese RA. Mass isotopomer distribution analysis at eight years: theoretical, analytic, and experimental considerations. Am J Physiol 1999;276:E1146. [PubMed: 10362629]
43. Appay V, Dunbar PR, Callan M, Klenerman P, Gillespie GM, Papagno L, Ogg GS, King A, Lechner F, Spina CA, Little S, Havlir DV, Richman DD, Gruener N, Pape G, Waters A, Easterbrook P, Salio

M, Cerundolo V, McMichael AJ, Rowland-Jones SL. Memory CD8+ T cells vary in differentiation phenotype in different persistent virus infections. Nat Med 2002;8:379. [PubMed: 11927944]

44. Champagne P, Ogg GS, King AS, Knabenhans C, Ellefsen K, Nobile M, Appay V, Rizzardi GP, Fleury S, Lipp M, Forster R, Rowland-Jones S, Sekaly RP, McMichael AJ, Pantaleo G. Skewed maturation of memory HIV-specific CD8 T lymphocytes. Nature 2001;410:106. [PubMed: 11242051]
45. Roederer M, Dubs JG, Anderson MT, Raju PA, Herzenberg LA, Herzenberg LA. CD8 naive T cell counts decrease progressively in HIV-infected adults. J Clin Invest 1995;95:2061. [PubMed: 7738173]
46. Asquith B, Debacq C, Macallan DC, Willems L, Bangham CR. Lymphocyte kinetics: the interpretation of labelling data. Trends Immunol 2002;23:596. [PubMed: 12464572]
47. Chang JT, Palanivel VR, Kinjyo I, Schambach F, Intlekofer AM, Banerjee A, Longworth SA, Vinup KE, Mrass P, Oliaro J, Killeen N, Orange JS, Russell SM, Weninger W, Reiner SL. Asymmetric T lymphocyte division in the initiation of adaptive immune responses. Science 2007;315:1687. [PubMed: 17332376]
48. Tough DF, Sprent J. Turnover of naive- and memory-phenotype T cells. J Exp Med 1994;179:1127. [PubMed: 8145034]
49. Schluns KS, Kieper WC, Jameson SC, Lefrancois L. Interleukin-7 mediates the homeostasis of naive and memory CD8 T cells in vivo. Nat Immunol 2000;1:426. [PubMed: 11062503]
50. Fry TJ, Connick E, Falloon J, Lederman MM, Liewehr DJ, Spritzler J, Steinberg SM, Wood LV, Yarchoan R, Zuckerman J, Landay A, Mackall CL. A potential role for interleukin-7 in T-cell homeostasis. Blood 2001;97:2983. [PubMed: 11342421]
51. Napolitano LA, Grant RM, Deeks SG, Schmidt D, De Rosa SC, Herzenberg LA, Herndier BG, Andersson J, McCune JM. Increased production of IL-7 accompanies HIV-1-mediated T-cell depletion: implications for T-cell homeostasis. Nat Med 2001;7:73. [PubMed: 11135619]
52. Hazenberg MD, Otto SA, van Benthem BH, Roos MT, Coutinho RA, Lange JM, Hamann D, Prins M, Miedema F. Persistent immune activation in HIV-1 infection is associated with progression to AIDS. Aids 2003;17:1881. [PubMed: 12960820]
53. Albuquerque AS, Cortesao CS, Foxall RB, Soares RS, Victorino RM, Sousa AE. Rate of increase in circulating IL-7 and loss of IL-7Ralpha expression differ in HIV-1 and HIV-2 infections: two lymphopenic diseases with similar hyperimmune activation but distinct outcomes. J Immunol 2007;178:3252. [PubMed: 17312174]
54. Boulassel MR, Mercier F, Gilmore N, Routy JP. Immunophenotypic patterns of CD8(+) T cell subsets expressing CD8alphaalpha and IL-7Ralpha in viremic, aviremic and slow progressor HIV-1-infected subjects. Clin Immunol 2007;124:149. [PubMed: 17560832]
55. Pahwa R, McCloskey TW, Aroniadis OC, Strbo N, Krishnan S, Pahwa S. CD8+ T cells in HIV disease exhibit cytokine receptor perturbation and poor T cell receptor activation but are responsive to gamma-chain cytokine-driven proliferation. J Infect Dis 2006;193:879. [PubMed: 16479523]
56. Colle JH, Moreau JL, Fontanet A, Lambotte O, Joussemet M, Delfraissy JF, Theze J. CD127 expression and regulation are altered in the memory CD8 T cells of HIV-infected patients--reversal by highly active anti-retroviral therapy (HAART). Clin Exp Immunol 2006;143:398. [PubMed: 16487237]
57. MacPherson PA, Fex C, Sanchez-Dardon J, Hawley-Foss N, Angel JB. Interleukin-7 receptor expression on CD8(+) T cells is reduced in HIV infection and partially restored with effective antiretroviral therapy. J Acquir Immune Defic Syndr 2001;28:454. [PubMed: 11744834]
58. Paiardini M, Cervasi B, Albrecht H, Muthukumar A, Dunham R, Gordon S, Radziewicz H, Piedimonte G, Magnani M, Montroni M, Kaech SM, Weintrob A, Altman JD, Sodora DL, Feinberg MB, Silvestri G. Loss of CD127 expression defines an expansion of effector CD8+ T cells in HIV-infected individuals. J Immunol 2005;174:2900. [PubMed: 15728501]
59. Rethi B, Fluur C, Atlas A, Krzyzowska M, Mowafi F, Grutzmeier S, De Milito A, Bellocco R, Falk KI, Rajnavolgyi E, Chiodi F. Loss of IL-7Ralpha is associated with CD4 T-cell depletion, high interleukin-7 levels and CD28 down-regulation in HIV infected patients. Aids 2005;19:2077. [PubMed: 16284456]

60. Okoye A, Meier-Schellersheim M, Brenchley JM, Hagen SI, Walker JM, Rohankhedkar M, Lum R, Edgar JB, Planer SL, Legasse A, Sylwester AW, Piatak M Jr, Lifson JD, Maino VC, Sodora DL, Douek DC, Axthelm MK, Grossman Z, Picker LJ. Progressive CD4+ central memory T cell decline results in CD4+ effector memory insufficiency and overt disease in chronic SIV infection. J Exp Med 2007;204:2171. [PubMed: 17724130]

61. Northfield JW, Loo CP, Barbour JD, Spotts G, Hecht FM, Klenerman P, Nixon DF, Michaelsson J. Human immunodeficiency virus type 1 (HIV-1)-specific CD8(+) T(EMRA) cells in early infection are linked to control of HIV-1 viremia and predict the subsequent viral load set point. J Virol 2007;81:5759. [PubMed: 17376902]

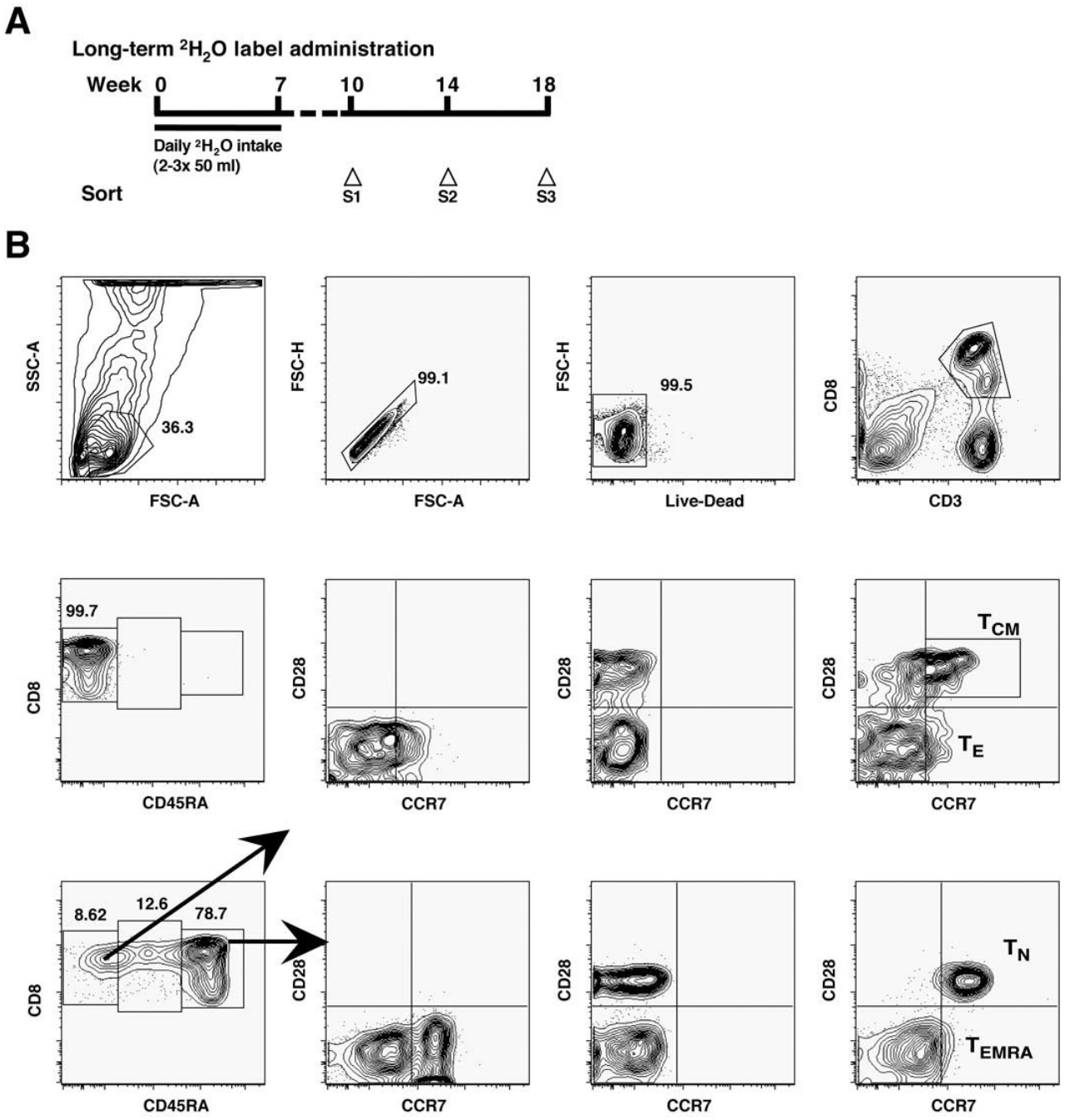

Figure 1.

In vivo stable isotope labeling protocol and gating strategy for T cell phenotyping. **(A)** Long-term ^2H_2O label administration. ^2H_2O was administered over a period of seven weeks (3 × 50 ml of 70% ^2H_2O per day during the first week and 2 × 50 ml of 70% ^2H_2O per day during the next six weeks). T cell subpopulations were sorted at three time points during the de-labeling phase: weeks 10 (S1), 14 (S2), and 18 (S3). **(B)** Flow cytometric gating strategy: Upper row from left to right: Lymphocytes were gated using forward scatter-area (FSC-A) versus side scatter-area (SSC-A). Doublets were excluded using FSC-A versus FSC-height (FSC-H). Live cells were negative for live/dead fixable aqua (Amine). $CD3^+CD8^+$ cells were gated. $CD8^{low}$ T cells were included in the gate. The fraction of $CD8^{low}$ T cells of total $CD8^+$ T cells

did not significantly differ between groups and also did not change significantly with lower CD4 counts. Middle row from left to right shows the FMOs (explained in Methods) for CD45RA, CD28, and CCR7, as well as the "all stain" (including all antibodies used for staining) for $CD3^{+}CD8^{+}CD45RA^{-}$ cells (farthest left gate in the lower left plot). The bottom row from left to right shows $CD45RA^{bright}$ (farthest right gate in the lower left plot), then the FMOs for CD28 and CCR7 as well as the "all stain" for $CD3^{+}CD8^{+}CD45RA^{bright}$ cells.

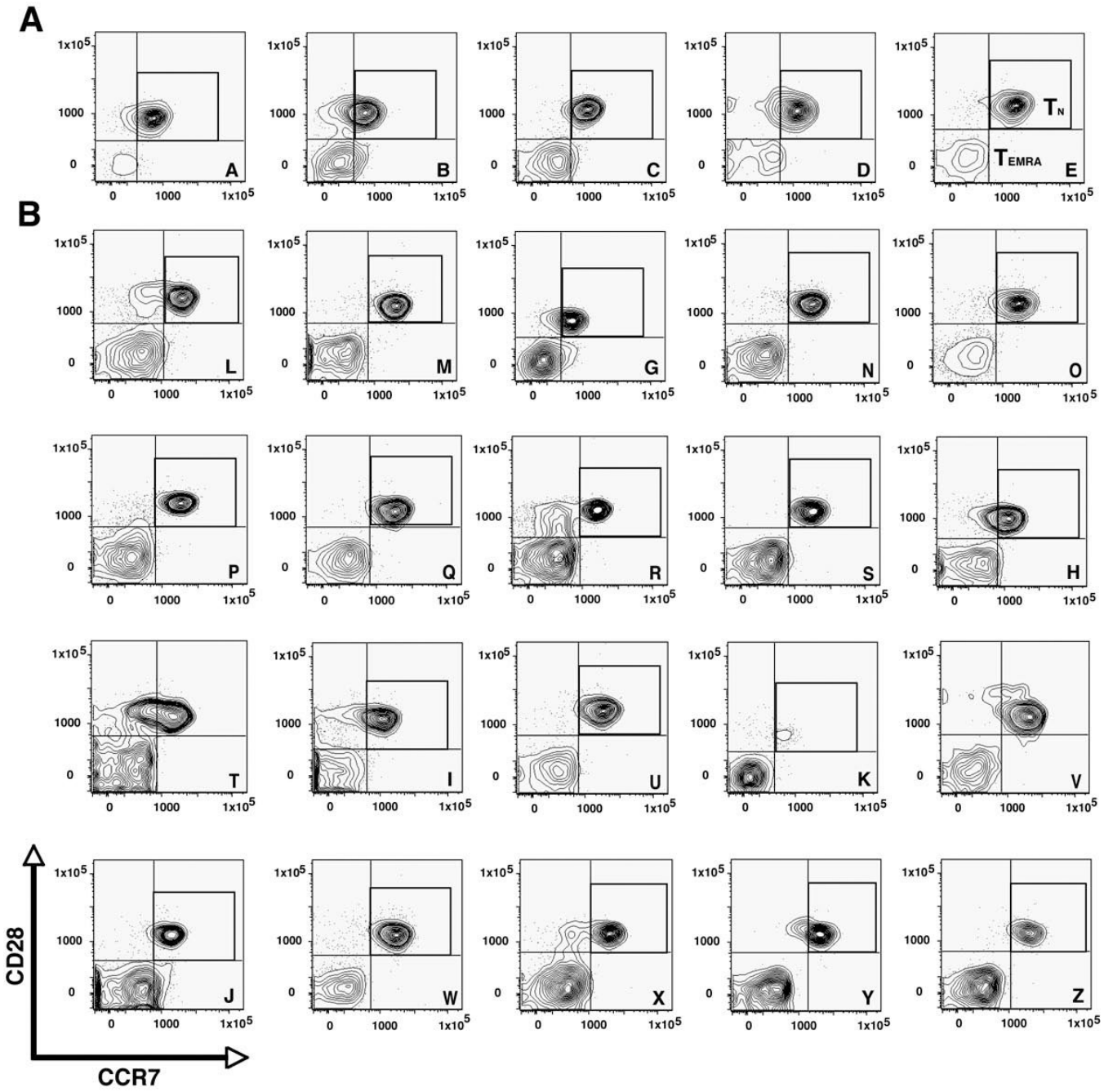

Figure 2.

Flow plots of $CD3^+CD8^+CD45RA^{bright}$ T cell subpopulations from the HIV-negative **(A)** and HIV-infected **(B)** subjects. The same gating strategy as in Figure 1, bottom row, was used with CCR7 on the x-axis and CD28 on the y-axis. The flow plots are shown with the location of the $CD3^+CD8^+CD45RA^{bright}CD28^+CCR7^+$ naïve T (T_N) cells and the $CD3^+CD8^+CD45RA^{bright}CD28^-CCR7^-$ RA effector T cells (T_{EMRA}) cells (labeled in the farthest right plot in (A)). Labels for T_N- and T_{EMRA} cell subpopulations are located on the right next to the respective gates. Gates for individual subjects were set based on FMO stains. The capital letters in the lower right corner of each plot correspond to the subject IDs listed in Table I and are displayed by decreasing CD4 count (from top left to bottom right).

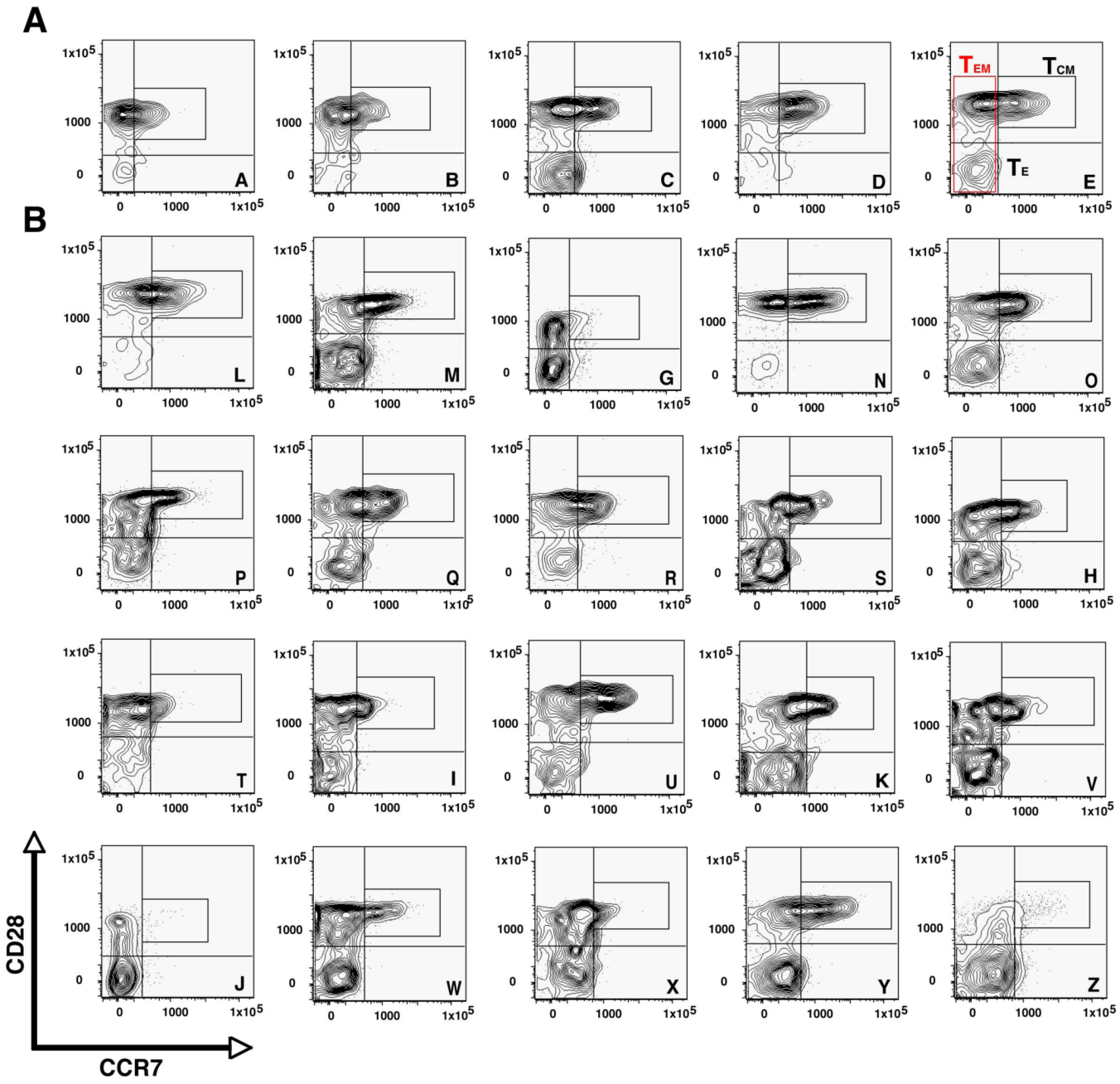

Figure 3.

Flow plots of $CD3^+CD8^+CD45RA^-$ T cell subpopulations from the HIV-negative **(A)** and HIV-infected **(B)** subjects. The same gating strategy as in Figure 1, middle row, was used with CCR7 on the x-axis and CD28 on the y-axis. The flow plots are shown with the location of $CD3^+CD8^+CD45RA^-CD28^+CCR7^+$ central memory T (T_{CM}) cells and $CD3^+CD8^+CD45RA^-CD28^-CCR7^-$ effector T (T_E) cells (labeled in the farthest right plot in (A)). Labels for T_{CM} and T_E cell subpopulations are located on the right next to the respective gates. Gates for individual subjects were set based on FMO stains. The capital letters in the lower right corner of each plot correspond to the subject IDs listed in Table I.

$CD8^+CD45RA^-CCR7^-$ T cells, which are here referred to as T_{EM} cells, are heterogeneous and consist of two distinct subpopulations when analyzed for expression of CD45RA, CCR7, and

CD28, namely CD45RA^{-}CCR7^{-}CD28^{+} as well as CD45RA^{-}CCR7^{-}CD28^{-} cells (red box around T_{EM} cells in (A), right flow plot in the upper row).

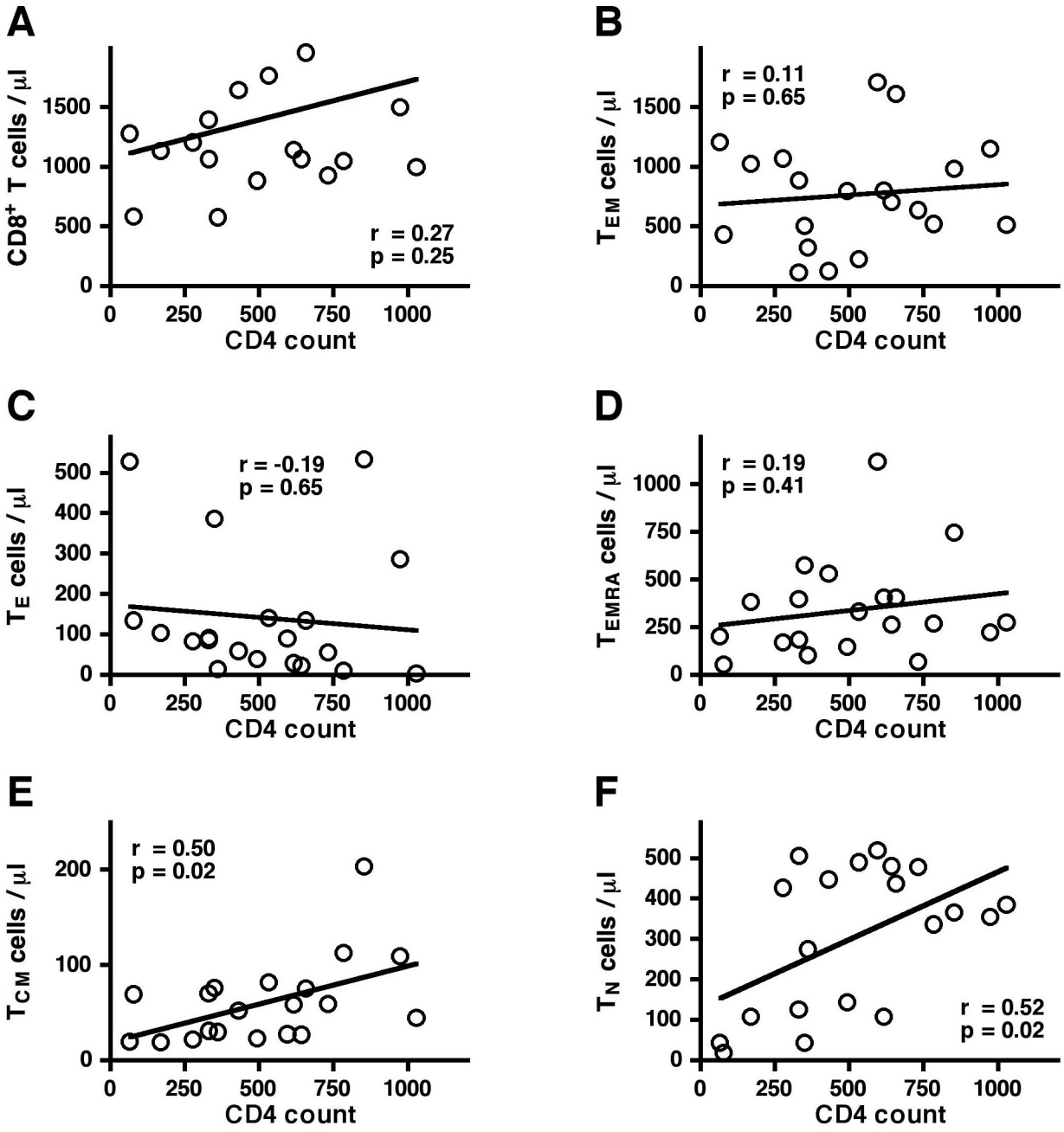

Figure 4.

Circulating $CD8^+$ T cell subpopulations in HIV-infected subjects. Linear regressions and Pearson correlations (calculated with 95% confidence intervals and two-tailed p values) between the circulating $CD4^+$ T cell count in HIV-infected patients (n = 20) and the absolute number of circulating **(A)** $CD8^+$ T cells, **(B)** T_{EM}, **(C)** T_E, **(D)** T_{EMRA}, **(E)** T_{CM}, and **(F)** T_N cells/µl. Pearson correlations are shown, as data sets were found to be normal as determined using the Kolmogorov-Smirnov normality test (see Methods).

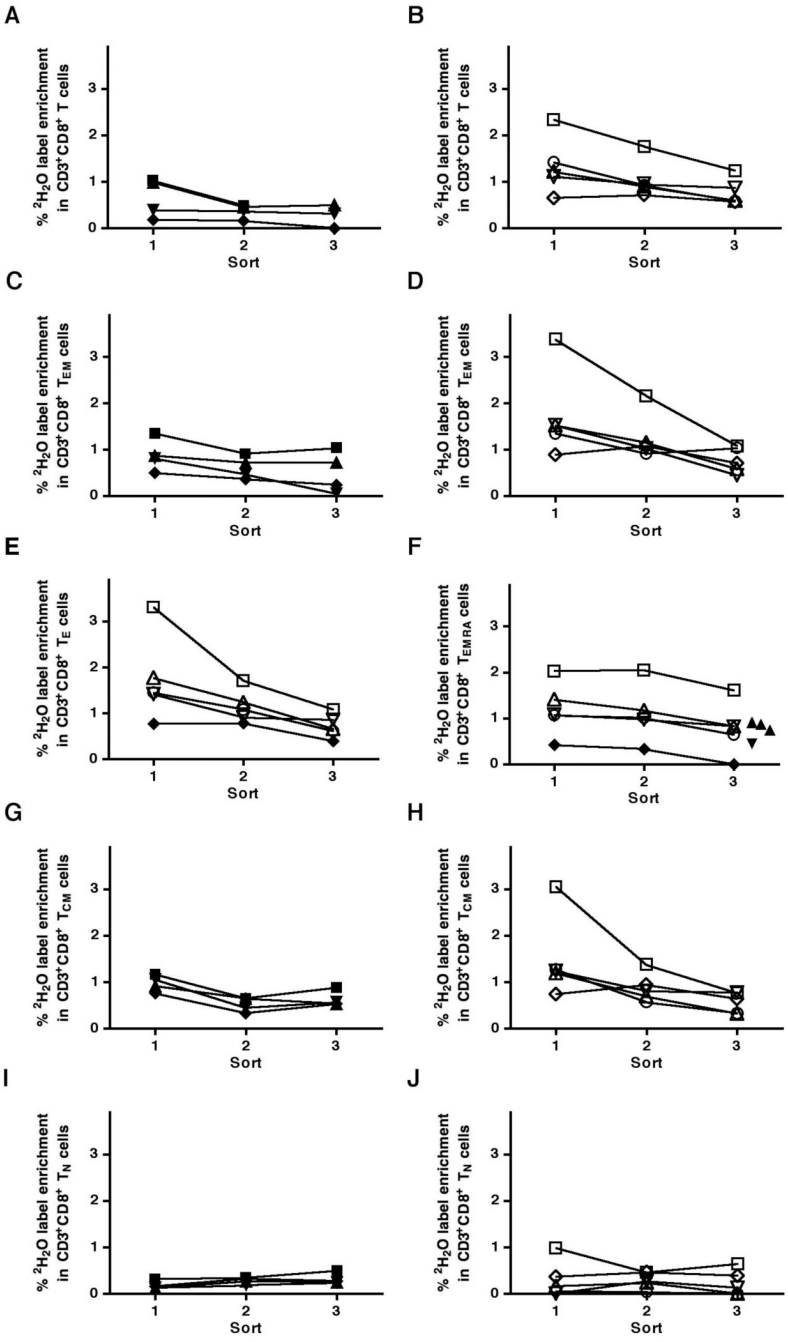

Figure 5.

Decay curves of ^2H_2O enrichment in DNA of different human $CD3^+CD8^+$ T cell subpopulations from HIV-negative (filled symbols) and HIV-infected (open symbols) subject following a seven week labeling protocol and three weeks of label wash-out from body water and during 8 weeks (week 10-18) of de-labeling for **(A, B)** $CD3^+CD8^+$ T cells, **(C, D)** T_{Em} cells, **(E)** T_E cells, **(F)** T_{Emra} cells, **(G, H)** T_{Cm} cells, and **(I, J)** T_N cells. In (E) and (F), data from both HIV-negative and HIV-infected subjects are shown in the same panel. The same symbols shown in the different panels are from the same subjects. The open squares are from the HIV-infected subject with the highest VL. The three triangles shown in (F) at S3 (shown next to each other to not overlap) represent ^2H_2O enrichments from three sorted T_{Emra} cell

samples from a single subject. The other filled symbols in (F) represent $^{2}H_{2}O$ enrichments from sorted T_{Emra} cell samples from other HIV-negative subjects.

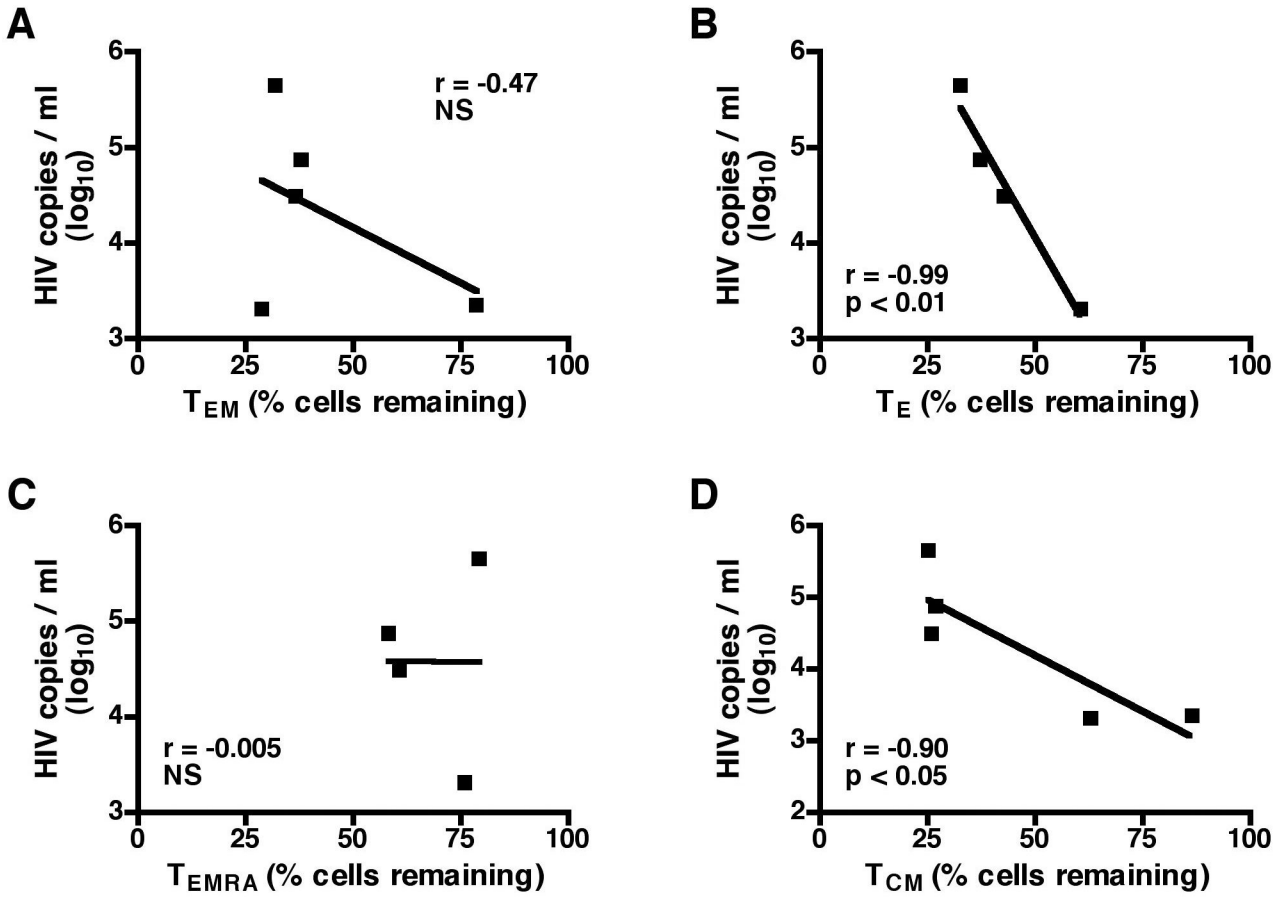

Figure 6.

Correlations between T_{EM}, $T_{E,}$ T_{EMra}, and T_{Cm} cells remaining and HIV VL. Linear regressions and correlations coefficient of the percentages of labeled **(A)** T_{EM} **(B)** T_{E} **(C)** T_{EMra} and **(D)** T_{Cm} cells per μl remaining at the end of the protocol (week 18) and HIV VL. In (B) and (C), only data from four of the five labeled HIV-infected subjects were available. Pearson correlations are shown, as data sets were found to be normal as determined using the Kolmogorov-Smirnov normality test (see Methods). NS not significant.

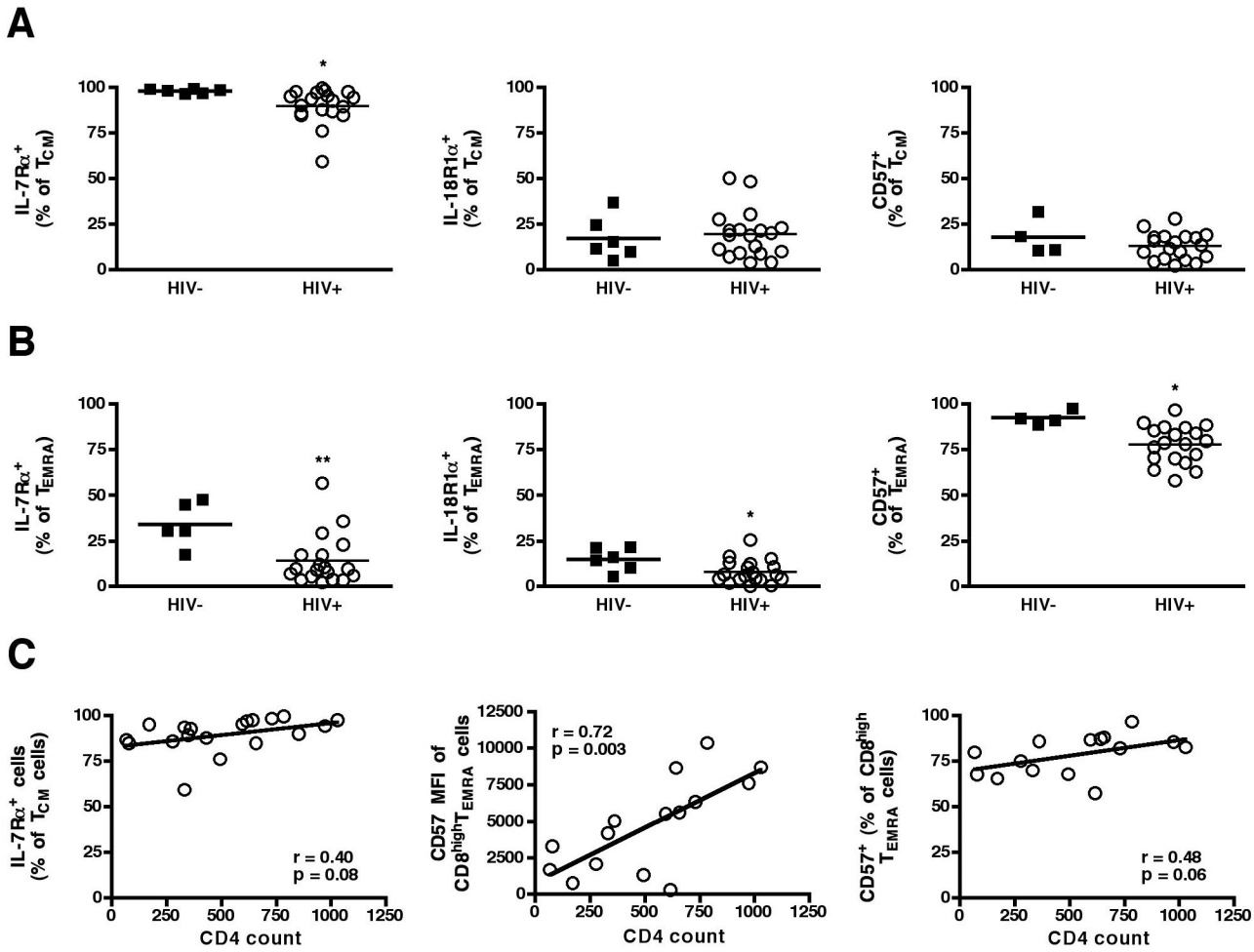

Figure 7.

Expression of IL-7Rα, IL-18R1α, and CD57 on T_{Cm} and T_{EMra} cells. **(A)** Percentages of T_{Cm} cells from HIV-negative or HIV-infected subjects expressing IL-7Rα (left), IL-18R1α (middle), or CD57 (right). **(B)** Percentages of T_{EMra} cells from HIV-negative or HIV-infected subjects expressing IL-7Rα (left), IL-18R1α (middle), or CD57 (right). **(C)** The relationship between CD4 count and the percentage of T_{Cm} cells expressing IL-7Rα (left), the MFI of CD57 on $CD8^{high}$ T_{EMra} cells (middle), and the percentage of $CD8^{high}$ T_{EMRA} cells expressing CD57 (right). * $p<0.05$ and ** $p<0.01$ HIV-negative versus HIV-infected (two-tailed Student's t test for comparisons between groups). The Student's t test was used for comparison between groups and Pearson correlations are shown, as data sets were found to be normal as determined using the Kolmogorov-Smirnov normality test (see Methods).

Table I

Characteristics of study subjects

Group	Subject ID	Age	VL (copies/ml)	Years HIV-infected	CD4 count / µl of blood	CD8 count / µl of blood	Weeks of ^2H_2O labeling
HIV-negative	A	27	Negative	-	586	376	7
	B	56	Negative	-	513	292	7
	C	59	Negative	-	555	488	7
	D	64	Negative	-	903	258	7
	E	35	Negative	-	1289	563	ND
	F	35	Negative	-	832	246	ND
HIV-infected (untreated)	L	41	< 75	5	1028	998	ND
	M	40	8278	9	973	1500	ND
	G	40	2,059	NA	852	3388	7
	N	52	713	5	784	1052	ND
	O	52	< 75	17	730	929	ND
	P	52	8469	16	657	1960	ND
	Q	52	< 75	11	642	1067	ND
	R	59	87	15	615	1143	ND
	S	38	392	13	594	2079	ND
	H	41	2,220	NA	532	1764	7
	T	42	6,897	11	493	884	ND
	I	38	30,851	NA	431	1646	7
	U	37	16,212	6	360	578	ND
	K	36	448,343	NA	349	2445	7
	V	41	17,090	11	331	1067	ND
	J	53	74,199	NA	330	1397	7
	W	46	32,236	11	277	1207	ND
	X	40	15,534	15	170	1133	ND
	Y	60	222,000	17	78	586	ND
	Z	47	467,160	21	66	1281	ND

ND not determined; NA not available

Table II

Information and results for $CD8^+$ T cell subpopulations from subjects labeled long-term (7 weeks) with ^2H_2O. The results shown are means ± SD.

$CD3^+CD8^+$ T cell subset	Group	HIV copies/ml) (log_{10})	k (decay constant)	$T_{1/2}$ (half-life in days)	Percentage of cells remaining	Cells/μl	% of $CD3^+CD8^+$ T cells
$CD45RA^-CCR7^-(CD28^{+/-})$ (T_{EM})							
	HIV-negative	-	0.0177 (± 0.0217)	105.8 (± 88.4)	53.7 (± 34.7)	31.3 (± 20.6)	9.7 (± 8.3)
	HIV-infected	4.3 (± 1.0)	0.0164 (± 0.0022)	35.9 (± 4.1)	42.8 (± 20.4)	391.7 (± 367.0)	15.7 (± 9.1)**
$CD45RA^-CCR7^-CD28^-$ (T_E)							
	HIV-negative	-	0.0119	58.1	51.3	8.3 (± 8.7)	2.2 (± 1.9)
	HIV-infected	4.3 (± 1.0)	0.0154 (± 0.0047)	49.3 (± 19.3)	43.3 (± 12.2)	241.4 (± 208.5)	9.9 (± 5.6)*
$CD45RA^+CCR7^-CD28^-$ (T_{EMRA})							
	HIV-negative	-	0.00007[A]	9762[A]	99.6[A]	33.2 (± 27.3)	8.9 (± 6.4)
	HIV-infected	4.3 (± 1.0)	0.0069 (± 0.0028)	114.5 (± 47.2)	68.5 (± 10.6)	515.9 (± 162.3)***	25.0 (± 5.3)**
$CD45RA^-CCR7^+CD28^+$ (T_{CM})							
	HIV-negative	-	0.0079 (± 0.0029)	97.7 (± 36.8)	64.9 (± 10.4)	30.5 (± 21.7)	9.15 (± 7.5)
	HIV-infected	4.3 (± 1.0)	0.0166 (± 0.0087)[B]	51.0 (± 30.4)[B]	45.5 (± 27.9)[B]	96.7 (± 60.6)	4.38 (± 1.2)
$CD45RA^+CCR7^+CD28^+$ (T_N)							
	HIV-negative	-	-[C]	-[C]	175.5 (± 16.1)	159.4 (± 82)	44.0 (± 18.6)
	HIV-infected	4.3 (± 1.0)	-[C]	-[C]	42.8 (± 52.0)**	294.7 (± 198.9)	15.3 (± 11.6)

* $p < 0.05$,

** $p < 0.01$,

*** $p < 0.001$ HIV-negative versus HIV-infected;

[A] To prevent underestimation, the ^2H_2O enrichment from the one subject at S1 and the mean ^2H_2O enrichment of three subjects at S3 were used to calculate "k", the half-life, and the percentage of cells remaining;

[B] $p<0.05$ HIV-negative versus HIV-infected high VL;

[C] Decay constants and half-lives for T_N cells could not be calculated, as label either increased during de-labeling (all of the HIV-negative subjects and the two HIV-infected subjects with low VL) or label could no longer be detected at the last time point during de-labeling (two of the HIV-infected subjects with high VL).